An N-Terminal EF Hand-like Motif Modulates Ion Transport by Pmr1, the Yeast Golgi Ca^{2+}/Mn^{2+}-ATPase†

Ying Wei, Valerie Marchi, Runsheng Wang, and Rajini Rao*

Department of Physiology, The Johns Hopkins University School of Medicine, 725 North Wolfe Street, Baltimore, Maryland 21205

Received May 17, 1999; Revised Manuscript Received August 5, 1999

ABSTRACT: Pmr1, a novel member of the family of P-type ATPases, localizes to the Golgi compartment in yeast where it provides Ca^{2+} and Mn^{2+} for a variety of normal secretory processes. We have previously characterized Ca^{2+} transport in isolated Golgi vesicles, and described an expression system for the analysis of Pmr1 mutants in a yeast strain devoid of background Ca^{2+} pump activity [Sorin, A., Rosas, G., and Rao, R. (1997) *J. Biol. Chem. 272*, 9895−9901]. Here we show, using recombinant bacterial fusions, that an N-terminal EF hand-like motif in Pmr1 binds Ca^{2+}. Increasing disruptions of this motif led to progressive loss of pump function; thus, the single point mutations D51A and D53A retained pump activity but with drastic reductions in the affinity for Ca^{2+} transport, while the double mutant was largely unable to exit the endoplasmic reticulum. In-frame deletions of the Ca^{2+}-binding motif resulted in complete loss of function. Interestingly, the single point mutations conferred differential affinities for transport of Ca^{2+} and Mn^{2+} ions. Further, the proteolytic stability of the catalytic ATP-binding domain is altered by the N-terminal mutations, suggesting an interaction between these two regions of polypeptide. These studies implicate the N-terminal domain of Pmr1 in the modulation of ion transport, and may help elucidate the role of N-terminal metal-binding sites of Cu^{2+}-ATPases, defective in Wilson and Menkes disease.

Cation pumps belonging to the ubiquitous P-ATPase superfamily share common structural and mechanistic features, including the formation of a catalytic phosphoenzyme intermediate and passage through at least two distinct conformational states designated E_1 and E_2. Well-known members of this family include the Ca^{2+}-ATPases, Na^+/K^+-ATPases, and H^+/K^+-ATPases of mammalian cells, and the H^+-ATPases of fungi and plants. For these members of the so-called P_2-subtype (*1*), there is now evidence from crystallographic as well as mutagenic studies for 10 membrane-spanning helices, of which 4 are clustered to form a putative transmembrane pore (*2*−*4*). The conserved ATP-binding and phosphorylation domains are located in the cytoplasm, between membrane spans 4 and 5. A smaller well-conserved cytoplasmic domain, composed primarily of antiparallel β-strands, lies between membrane spans 2 and 3, and is known to be important in the conformational changes from E_1 to E_2 (*5*). The cytoplasmic amino and carboxy termini are widely divergent in sequence, with the latter having regulatory elements in a number of cation pumps (*6, 7*). However, the specific function of the N-terminal stretch of polypeptide, if any, is less clear. Strikingly, in the Cu^{2+}-, Cd^{2+}-, and Zn^{2+}-transporting ATPases of the P_1-subtype, there are tandem repeats of metal-binding motifs within an extended N-terminus, which have been implicated in functioning either as a metal ion 'sensor' or in the delivery of ions to the translocating pore (*8*). Progressive mutagenesis of the six Cu^{2+}-binding motifs in the Cu^{2+}-ATPase defective in Menkes disease resulted in a precipitous loss of function following disruption of the third site, as judged by the assay of Cu^{2+}-dependent Fet3 oxidase activity in yeast (*9*), and a loss of copper-induced traffic to the plasma membrane (*34*). However, in the absence of direct measurements of copper transport by mutant ATPases, it is difficult to assign a specific role for the ion-binding motifs.

The yeast Golgi Ca^{2+},Mn^{2+}-ATPase Pmr1 has a putative Ca^{2+}-binding EF hand-like motif within its N-terminal stretch of polypeptide (*10, 11*). The EF hand is a helix−loop−helix motif in which a central Ca^{2+} ion is chelated by oxygen atoms arranged along the *X*, *Y*, and *Z* coordinates (reviewed in *12, 32*). Proteins containing EF hands may act as sensors of intracellular calcium levels, such as calmodulin and troponin C, or may serve as calcium buffers, as exemplified by parvalbumin. Putative EF hands have also been identified in Ca^{2+}-activated K^+ and Ca^{2+} channels, including the ryanodine receptor, and the plant KCO1 channel (*13, 14*), where they are thought to confer Ca^{2+} sensitivity. A point of caution, however, is that it is difficult to predict from amino acid sequence alone whether a given EF hand motif binds Ca^{2+}, and variations in the 12-residue consensus loop can alter Ca^{2+}-binding affinities drastically (K_d between 10^{-4} and 10^{-9} M). Unlike classical EF hand domains, the putative Ca^{2+}-binding motif in Pmr1 is unpaired, and its role, if any, is unknown.

† This work was supported by grants from the American Cancer Society (IRG11-33 and JFRA 538), the American Heart Association (Grant-In-Aid 95012290), and the National Institutes of Health (GM52414) to R.R., by a Provost Award for Undergraduate Research by the The Johns Hopkins University to V.M., and by a Visiting Scholar Award from the World Health Organization to R.W.

* To whom correspondence should be addressed. Phone: (410) 955-4732. Fax: (410) 955-0461. E-mail: rrao@jhmi.edu.

10.1021/bi9911233 CCC: $18.00
Published on Web 10/14/1999

In this study, we provide evidence that the N-terminal domain of Pmr1, fused to bacterial GST,[1] does indeed bind Ca^{2+}. We then examine the effects of substitutions and deletions in the Ca^{2+}-binding motif on Ca^{2+} pump expression and localization, polypeptide stability, and Ca^{2+} and Mn^{2+} transport. The results suggest that the N-terminus of Pmr1 plays a hitherto unrecognized role in transport, perhaps via conformational interactions with the catalytic domain.

EXPERIMENTAL PROCEDURES

Media, Strains, Growth Assays. Yeast strains were grown in defined media containing yeast nitrogen base (6.7 g/L; Difco), dextrose (2%), and supplements as needed. *PMR1*-containing plasmids were introduced into strain K616 (*15*), which carries null alleles of calcineurin B (*CNB1*) and two Ca^{2+}-ATPases (*PMR1* and *PMC1*), resulting in low basal Ca^{2+} pump activity, as previously described (*11*). Growth assays were performed by inoculating 1 mL of YNB medium in a multiwell plate with 2−5 μL of a saturated seed culture. $MnCl_2$ was added at the concentrations indicated, and growth was monitored by measuring absorbance at 600 nm after culturing for 48 h at 30 °C.

Plasmids and Mutagenesis. YEpHR1, a yeast 2μ plasmid carrying the *PMR1* coding sequence under control of a tandem repeat of a yeast heat shock element, has been described previously (*11*). A series of in-frame deletions were introduced within the N-terminal sequence of *PMR1* in this plasmid, as follows. A 300 base pair *Hin*dIII−*Bam*HI fragment of *PMR1* was introduced into pUC19 and linearized at the *Xba*I site immediately proximal to the region encoding the EF hand motif. Digestion with exonuclease III was used to generate limited deletions at the termini, following which the termini were repaired with mung bean nuclease and ligated. Four in-frame deletions of 48, 60, 108, and 132 base pairs, respectively (Figure 1), were verified by sequencing the *Hin*dIII−*Bam*HI fragment, and introduced into the expression vector YEpHR1 using standard cloning techniques. To insert a polyhistidine tag at the N-terminus of Pmr1, the initiation ATG codon was replaced with a unique *Mlu*I site using the primers 5′-GATAAGATAATTACGCGTGACAATCC-3′ and 5′-AGTGTGATACTAACAGC-3′ (oPMR1−7), in conjunction with the polymerase chain reaction (base substitutions underlined). The amplified product (350 base pairs) was digested with *Mlu*I and *Bam*HI, and joined to a *Bam*HI−*Sac*II fragment of *PMR1* (2.2 kilobase pairs) and a *Mlu*I−*Sac*II fragment of plasmid pSM1052 (7.6 kilobase pairs; gift of Susan Michaelis, Johns Hopkins University) via a three-part ligation. To complete reconstruction of the 3′ region of the *PMR1* gene, a *Sac*II−*Sac*I fragment (1.2 kilobase pairs) was cloned into the above plasmid, resulting in a new expression plasmid, named YEpHisPMR1. This is a 2μ-based plasmid with the *URA* selectable marker, in which *PMR1* gene expression is directed from the constitutive *PGK* promoter. Amino acid substitutions within the EF hand motif were introduced into YEpHisPMR1 by the polymerase chain reaction, using the megaprimer method (*16*) as modified (*17*). The following oligonucleotides were used: Asp51→Ala (5′-GAAAAACTGGCCACTGACAAAAAC-3′), Asp53→Ala (5′-CTGGACACTGCCAAAAACGGT-3′), and Asp51,53→Ala (5′-GAAAACTGGCCACTGCCAAAAACGGTG-3′), in conjunction with the antisense primer oPMR1−7, described above. In each case, the amplified fragment was entirely sequenced to rule out unwanted mutations. Reconstruction of the mutagenized fragments into plasmid YEpHisPMR1 was by standard cloning techniques.

Fusion of the N-terminal 75 amino acids of Pmr1 with *Schistosoma japonicum* glutathione *S*-transferase was accomplished using the vector pGEX-4T-2 (Pharmacia Biotech) as follows. Wild-type or mutant *PMR1* sequences were amplified using the following pair of oligonucleotides: 5′-GTTCCGCGTGGATCCCCGGGTATGAGTGACAATCCATTT-3′ and 5′-CGCTCGAGTCGACCCTCATTCATTGGGGCCATAAAG-3′. The PCR product was digested with *Bam*HI and *Sal*I, and cloned into pGEX-4T-2. Note that the Pmr1 sequences lacked a His tag. Plasmids were introduced into *E. coli* strain BL21.

Cell Fractionation, Preparation of Membranes, and GST-Fusions. Preparations of total membranes, subcellular fractionation by sucrose gradient centrifugation, and isolation of Golgi vesicles from yeast were exactly as described earlier (*11*). Isolation of recombinant GST-fusion proteins was done essentially as per manufacturers' protocols (Pharmacia). Briefly, bacteria were cultured to mid-logarithmic phase at 37 °C and induced with IPTG (0.1 mM) for 2 h before being harvested. Cells were lysed by sonication in phosphate-buffered saline (PBS) containing protease inhibitors (*11*). Following removal of cell debris by low-speed centrifugation, the lysate was incubated with glutathione−Sepharose 4B (10 min), washed with PBS, and eluted with 50 mM Tris-HCl buffer, pH 8.0, containing 10 mM reduced glutathione. To minimize proteolysis of the fusion proteins, all steps were conducted at 0−4 °C for minimal times.

$^{45}Ca^{2+}$ Transport and Overlay Assays. ATP-dependent ^{45}Ca transport assays of sucrose gradient fractions and pooled Golgi membranes were done by rapid filtration as described previously (*11*). Concanamycin A (Sigma; 10 nM) and CCCP (25 μM) were added to eliminate the activity of vacuolar H^+/Ca^{2+} exchange. Titrations of calcium were conducted in buffer containing 10 mM Hepes/NaOH, pH 6.7, 0.15 M KCl, 5 mM $MgCl_2$, 0.5 mM ATP, 5 mM NaN_3, 25 μM CCCP, 50 nM concanamycin A, and $^{45}CaCl_2$ at a concentration of 15−20 μM and specific activity of 2 μCi/mL. Free calcium was varied by addition of EGTA, as calculated by the computer program of Fabiato and Fabiato (*18*). In assays of Mn^{2+} competition, ^{45}Ca was at 0.4 μCi/mL (nominally, 0.8 μM) and $MnCl_2$ was added as indicated.

Calcium binding to recombinant GST-fusion proteins was measured using a ^{45}Ca overlay assay essentially as described (*19*), with the following modifications. Approximately equal amounts of immunoreactive fusion protein, purified as described above, were slot-blotted onto nitrocellulose (0.45 μm, Schleicher & Schuell). Membranes were briefly dried and rinsed in a solution of 145 mM NaCl and 5 mM sodium phosphate, pH 7.4, and then in a solution of 10 mM imidazole, 100 mM KCl, pH 6.8. Following a 10 min incubation in the latter buffer supplemented with $^{45}CaCl_2$ at 1 μCi/mL (6.72 μCi/μg; ICN Biomedicals), the membrane

[1] Abbreviations: GST, glutathione *S*-transferase; SERCA, sarco/endoplasmic reticulum Ca^{2+}-ATPase; PMCA, plasma membrane Ca^{2+}-ATPase; CCCP, carbonyl cyanide *m*-chlorophenylhydrazone; SDS, sodium dodecyl sulfate; PAGE, polyacrylamide gel electrophoresis.

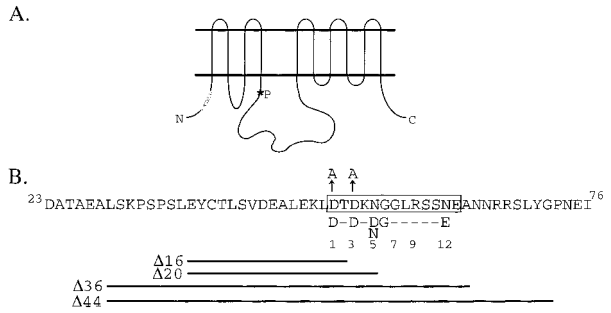

FIGURE 1: EF hand-like motif of Pmr1. (A) Topological model of the Ca^{2+}-ATPase with both N- and C-termini and the major extramembranous loops located in the cytoplasm. The region of the EF hand motif (in gray) and the site of the aspartyl phosphate reaction intermediate (*P) are shown for reference. (B) Sequence of the N-terminal region, with the EF loop *boxed*. Consensus residues and their loop positions are shown below the box. The substitutions (D→A) and four in-frame deletions used in this study are shown.

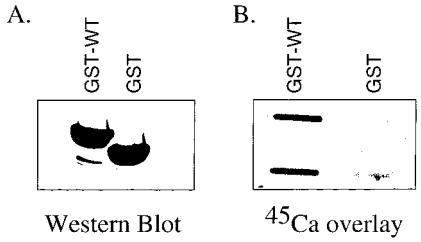

FIGURE 2: Calcium binding by GST−EF domain fusion. (A) Western blot of 20 μg each of purified GST and a fusion of the N-terminal 75 amino acids of Pmr1 with GST (GST-WT), probed with anti-GST antibody, as described under Experimental Procedures. (B) Autoradiograph of a slot blot in which equimolar amounts (1.5 nmol) of the purified proteins shown in panel A were deposited on nitrocellulose, in duplicate, and overlaid with $^{45}CaCl_2$ (1 μCi/mL) as described under Experimental Procedures. One of several independent experiments, showing ^{45}Ca binding by the Pmr1 fusion, but not the control, is shown.

was rinsed with water, dried thoroughly, and exposed to film for autoradiography.

Trypsinolysis. Pooled Golgi membranes (1 mg/mL) were incubated at 25 °C in buffer containing 20 mM Tris-HCl, pH 7.0, 0.1 M KCl, 5 mM $MgCl_2$, and treated with trypsin (TPCK treated, Sigma) at a trypsin:protein ratio of 1:8. Na_2-ATP (pH 6.7) was added at 5 mM, when specified. At the indicated times, the digests were terminated by addition of trichloroacetic acid to 10%. Samples were incubated on ice (30 min) and collected by microcentrifugation (30 min), and the resulting pellets were resuspended in gel loading buffer (*21*) for electrophoresis.

Protein Assays, Gel Electrophoresis, and Western Blotting. Protein concentration was determined by a modified Lowry assay (*20*) following precipitation of samples containing sucrose by 10% trichloroacetic acid, and using bovine serum albumin as standard. Samples were prepared for electrophoresis by precipitating with trichloroacetic acid as described (*11*). SDS−PAGE and Western blotting were performed as described previously (*21*). Western blots were scanned and quantitated using MacBAS (v. 2.31). Antibodies against the C-terminal one-third of PMR1 have been described previously (*11*); anti-GST antibodies were purchased from Pharmacia Biotech and used at a dilution of 1:1000.

RESULTS

Fusion of the N-Terminal Domain of Pmr1 with Glutathione S-Transferase Binds Ca^{2+}. Inspection of the predicted secondary structure of the N-terminal sequence of Pmr1 revealed a helix−loop−helix region having several of the consensus residues characteristic of the EF hand motif, as shown in Figure 1. In a typical EF hand, residues at positions 1, 3, 5, 7, 9, and 12 are known to contribute Ca^{2+}-liganding groups that lie along the $+X$, $+Y$, $+Z$, $-X$, $-Y$, and $-Z$ coordinates, respectively. Aspartate, glutamate, or asparagine residues occupy most of these positions in Pmr1. In EF hands of known structure, the glutamate residue at position 12 resides on the α-helix following the loop, and provides a bidentate ligand for the calcium ion. A notable difference in the Pmr1 sequence is the insertion of an additonal glycine in the loop, resulting in the displacement of the consensus glutamate to position 13. It was therefore important to directly assess the Ca^{2+}-binding ability of the N-terminal motif in Pmr1.

Initial attempts to express the first hundred amino acids of Pmr1, extending from the N-terminus to a unique *Bam*HI restriction site in the middle of the first predicted transmembrane segment, as a C-terminal fusion with glutathione *S*-transferase resulted in a proteolytically labile polypeptide. This seemed likely due to the destabilizing effects of the hydrophobic residues at the end of the fusion protein. The presence of a stable proteolytic polypeptide of ca. 35 kDa in the initial preparations was indicative of a smaller, independently folded domain. This observation led to the design of a stable fusion protein, containing the first 75 amino acids of Pmr1, that could be readily purified to homogeneity. We used a nonequilibrium filter-binding assay to detect Ca^{2+} binding by the putative EF hand-like motif (*19*). Equimolar amounts of purified fusion protein and the control GST were deposited on nitrocellulose filters and incubated with 5 μM $^{45}CaCl_2$, as described under Experimental Procedures. Figure 2 demonstrates the ability of the purified GST−Pmr1 fusion protein to bind ^{45}Ca, relative to the control glutathione *S*-transferase polypeptide. Addition of molar excess of Mn^{2+} (5 mM) to the binding assay abolished Ca^{2+} binding, while Mg^{2+} (5 mM) was less effective (not shown).

Substitutions and Deletions in the EF Hand-like Motif of Pmr1 Cause Progressive Loss of Function

To probe the function of the Ca^{2+}-binding EF hand-like domain of Pmr1, we made individual and combined substitutions of the aspartate residues at putative loop positions 1 and 3 to alanine (D51A and D53A, respectively). These substitutions were incorporated into a $(His)_9$-tagged Pmr1 polypeptide, for future purification of the ATPase. In addition, we examined the effects of four in-frame deletions within the N-terminal Pmr1 sequence, extending into the EF hand motif, as indicated in Figure 1. Wild-type, His-tagged, and mutant Pmr1 ATPases were expressed in a yeast strain devoid of background Ca^{2+} pump activity (K616; Δ*pmr1*Δ*pmc1*Δ*cnb1*), as described earlier (*11*). The effects of the substitutions and deletions are summarized below.

(i) Expression Levels. Quantitation of Pmr1 expression levels in preparations of yeast total membranes provided an initial estimate of the stability of the mutant polypeptides. On average, all mutants were expressed at levels of 60% or

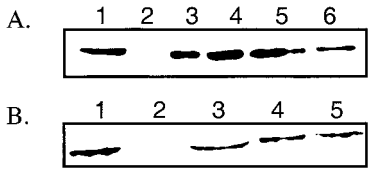

FIGURE 3: Western analysis of the expression levels of Pmr1 polypeptides. 10 μg of total membrane protein isolated from Δ*pmc1*Δ*pmr1*Δ*cnb1* yeast transformed with wild-type or mutant Pmr1 was separated on SDS−PAGE, immunoblotted, and probed with polyclonal anti-Pmr1 antibody as described under Experimental Procedures. (A) Lane 1, wild-type Pmr1; lane 2, host strain with no Pmr1; lanes 3−6, deletion mutants Δ16, Δ20, Δ36, and Δ44, respectively. (B) Lane 1, $(His)_9$-tagged Pmr1; lane 2, host strain with no Pmr1; lanes 3−5, $(His)_9$-tagged mutants D51A, D53A, and D51,53A, respectively.

greater, relative to wild type, as quantitated by densitometric scans of the Western blots. A representative set of membrane preparations is shown in Figure 3.

(ii) Golgi Localization. Mutant polypeptides that fail to pass cellular quality control are retained in the endoplasmic reticulum, presumably due to folding defects. The subcellular localization of the Pmr1 mutants was determined by fractionating yeast lysates on a 10-step sucrose density gradient. We have previously demonstrated that the lighter Golgi membranes (26−34% sucrose) are well separated from the endoplasmic reticulum, which is distributed in the denser half of this gradient (42−54% sucrose; ref *11*). Here we show that both wild-type and His-tagged Pmr1 are correctly localized to the Golgi, as are the D51A and D53A point mutants, whereas the double point mutant and the deletion mutants are partly retained in the endoplasmic reticulum (Figure 4). However, in each case, there was sufficient Golgi expression to be able to evaluate the transport activity of the pump (see below), suggesting that exit of the mutant polypeptides from the endoplasmic reticulum was delayed, rather than arrested.

(iii) ^{45}Ca Transport. Individual fractions from the sucrose gradients described above were assayed for ATP-dependent ^{45}Ca transport activity in the presence of protonophores and inhibitors of vacuolar H^+/Ca^{2+} exchange. In the absence of endogenous Ca^{2+} pumps in the host strain (Δ*pmc1*Δ*pmr1*Δ*cnb1*; K616), Ca^{2+} pumping activity is entirely dependent on the activity of plasmid-borne Pmr1, and is restricted to the Golgi-containing fractions. As shown in Figure 4, there was no $^{45}Ca^{2+}$ transport activity detected above the vector-transformed control in any of the deletion mutants, indicative of a complete loss of transport function. His-tagged Pmr1 (Figure 4B) was found to have activity comparable to the untagged version (Figure 4A), suggesting that pump function was uncompromised by introduction of the N-terminal nine histidine residues. Golgi fractions containing the D51A and D53A mutants had about one-third of normal activity; however, after compensation for the decreased expression levels, greater than 50% activity was found to be retained. The drastic loss of Golgi expression of the D51,53A double mutant made it difficult to quantitate residual activity (Figure 4B).

We conclude from this initial analysis that deletion of part or all of the helix−loop−helix region results in complete loss of function, indicating either a structural requirement for this domain or a strict requirement for N-terminal Ca^{2+} binding, in transport. Loss of the individual aspartates at positions 51 and 53 did not abolish Ca^{2+} transport activity of the pump, although the double mutant had a more severe effect.

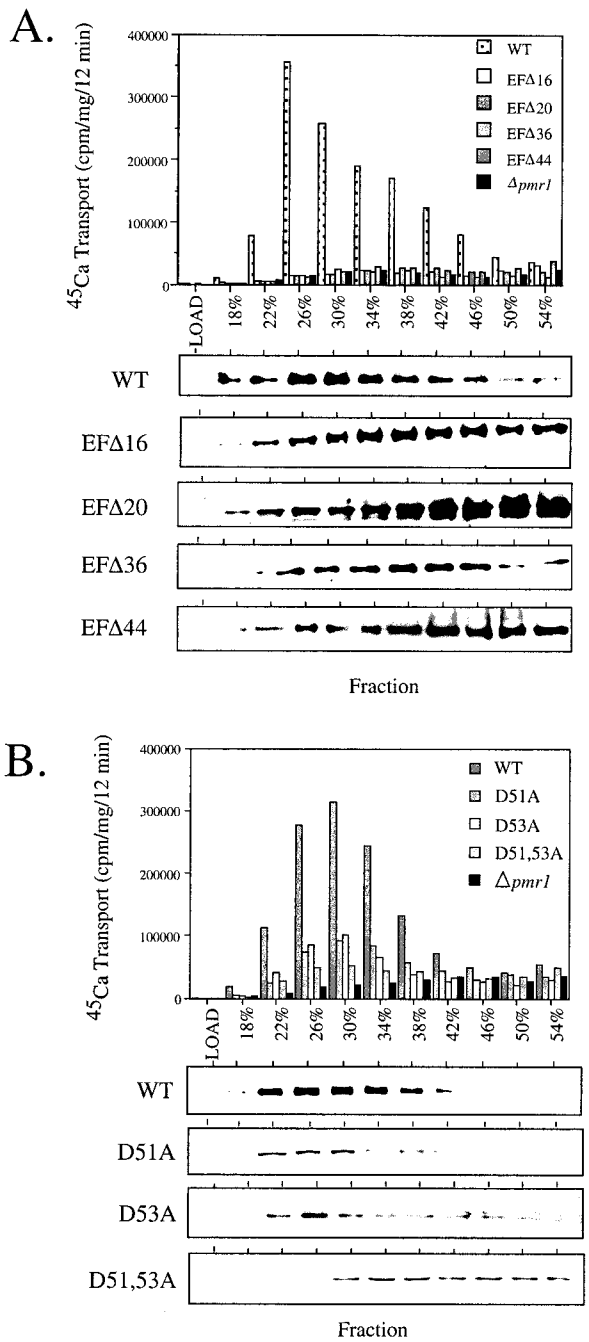

FIGURE 4: Calcium transport activity and subcellular localization of Pmr1 polypeptides. Yeast lysates were fractionated on a 10-step sucrose gradient (18−54%), and the individual fractions were assayed for Pmr1 pump activity and expression as described under Experimental Procedures. Golgi membranes peak at 26−34% sucrose, while the endoplasmic reticulum is found between 42 and 54% sucrose (*11*). 20 μg of each fraction was separated on SDS−PAGE, transferred to nitrocellulose, and probed with polyclonal anti-Pmr1 antibody. Each panel shows data from fractionation of control and Pmr1 mutant strains, as indicated. (A) Wild-type Pmr1, deletion mutants, and the Δ*pmr1* host strain. (B) $(His)_9$-tagged Pmr1 and the corresponding tagged point mutations.

Differential Effects of the Point Mutations D51A and D53A on Cation Affinity

Substitution of the aspartates at positions 51 and 53 had similar effects on the biogenesis of the ATPase, and on the

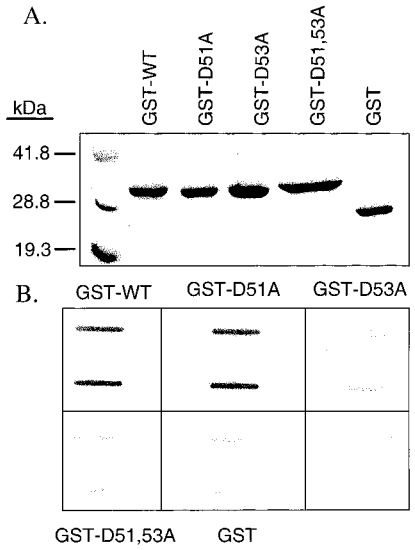

FIGURE 5: Isolation and calcium-binding ability of Pmr1−GST fusions. (A) 5 μg of purified wild-type (GST-WT) and mutant Pmr1−GST fusions was separated by SDS−PAGE and stained with Coomassie Blue. At the extreme left are molecular mass markers, as indicated, and at the extreme right is purified GST. (B) Equimolar amounts (0.8 nmol) of purified GST or GST fusion proteins were deposited in duplicate on nitrocellulose, by slot-blotting, and overlaid with $^{45}CaCl_2$ (1 μCi/mL) as described under Experimental Procedures. Blots were washed, dried, and subjected to autoradiography.

transport activity measured in the sucrose gradient fractions (Figures 3 and 4B). However, upon further analysis, the two mutations were found to have large and distinctly different effects on the affinities for Ca^{2+} and Mn^{2+} ions, as inferred by the experiments described ahead.

(i) Ca^{2+} Binding by GST-Fusions. The single and double point mutations were introduced into fusions of the N-terminal domain with glutathione-*S*-transferase, which were purified to homogeneity (Figure 5 A). Slot blots of equimolar amounts of the control and mutant fusion proteins were overlaid with ^{45}Ca to provide a qualitative estimate of calcium binding (Figure 5B). It was apparent that under the binding conditions used, calcium binding was retained in the D51A mutant but reduced below the level of detection by the overlay assay in the D53A and D51,53A mutants. Although this assay is not amenable to quantitative determination of affinities, the results indicate that the aspartate at position 53 is critical for Ca^{2+} binding, but that of position 51 is not.

(ii) K_M for ^{45}Ca Transport. Peak Golgi-containing fractions from sucrose density gradients were pooled and collected by centrifugation as described (*11*). ^{45}Ca transport into isolated Golgi vesicles was assayed as a function of free Ca^{2+} concentration, and the half-maximal concentration of Ca^{2+} required for transport was determined as described in Figure 6. The K_M for Ca^{2+} in the His-tagged Pmr1 control was 0.07 $\pm$ 0.01 μM, essentially as reported earlier for untagged Pmr1 (*11*). The affinity for Ca^{2+} was shifted nearly 8-fold to 0.52 $\pm$ 0.1 μM in the D51A mutant, and 11-fold to 0.77 $\pm$ 0.2 μM in the D53A mutant. The large decreases in the Ca^{2+} affinities are striking, considering that the mutations are in the cytoplasmic N-terminal domain, and quite distal in primary structure from the transmembrane segments involved in Ca^{2+} transport.

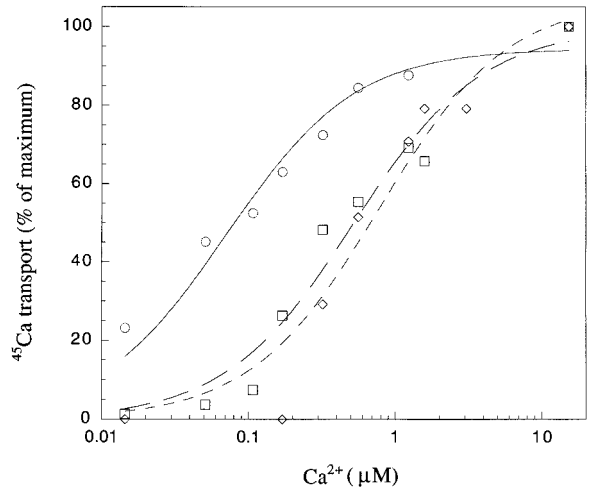

FIGURE 6: Calcium dependence of the transport activity of Pmr1. Pooled Golgi membranes were assayed for ^{45}Ca transport as a function of free [Ca^{2+}], buffered with EGTA, as described in the text. Symbols are as follows: ○, $(His)_9$-tagged Pmr1; □, D51A; and ◊, D53A. One of three independent experiments is shown. Data points were fit to the equation: $v = V_{max}S/(K_M + S)$ using Kaleidagraph, and had an r value of 0.98 in each case. The derived values for K_M are reported in the text.

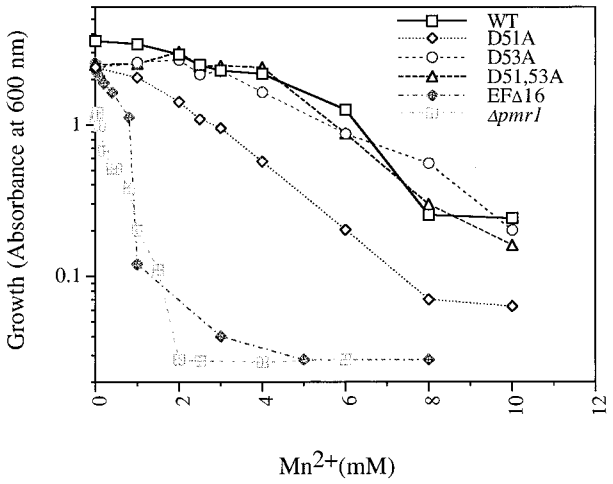

FIGURE 7: Manganese-tolerant growth in yeast strains expressing wild-type or mutant Pmr1. Yeast growth, in medium supplemented with the indicated amounts of $MnCl_2$, was monitored after incubation at 30 °C until saturation was reached (48 h), as described under Experimental Procedures. The Mn^{2+}-sensitive growth of the EFΔ16 mutant closely followed that of the Δ*pmr1* host strain (K616), and was representative of all deletion mutants. Data are representative of one of three independent experiments, which agreed closely.

(iii) Mn^{2+} Toxicity. Pmr1 has been proposed to function as a Mn^{2+} pump based on observations that *pmr1* mutants accumulate cytosolic Mn^{2+} and show Mn^{2+}-related glycosylation defects (*22*, *23*). Manganese is an essential ion for yeast growth, but becomes toxic at higher concentrations (*31*). Because *pmr1* mutants are hypersensitive to Mn^{2+}, it appears that the major route of Mn^{2+} detoxification is transport into the Golgi and exit via the exocytic pathway (*22*). We reasoned that growth in Mn^{2+}-containing media would be a measure of the Mn^{2+} transport activity of Pmr1. Titration of Mn^{2+} toxicity in strains expressing wild-type or mutant Pmr1 is shown in Figure 7. The deletion mutants, as exemplified by the ΔEF16 mutant in Figure 7, showed no improvement in Mn^{2+} tolerance above the Δ*pmr1* background. This suggested a loss of Mn^{2+} transport in these

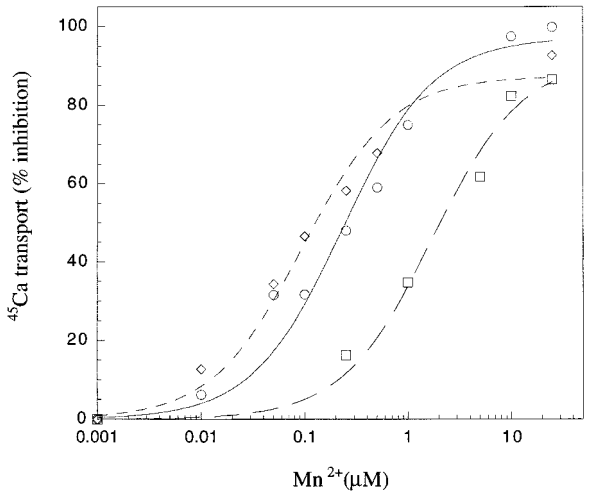

FIGURE 8: Manganese inhibition of calcium transport. ^{45}Ca transport in peak Golgi fractions of sucrose density gradients was measured in the presence of the indicated amounts of $MnCl_2$, as described under Experimental Procedures. Control samples contained no $MnCl_2$. Symbols are as in Figure 6. Data points are averages of duplicates; one of two independent experiments is shown. Data were fitted as described in the legend to Figure 6, and had an r value of 0.99 in each case. The derived values for $K_{0.5}$ are reported in the text.

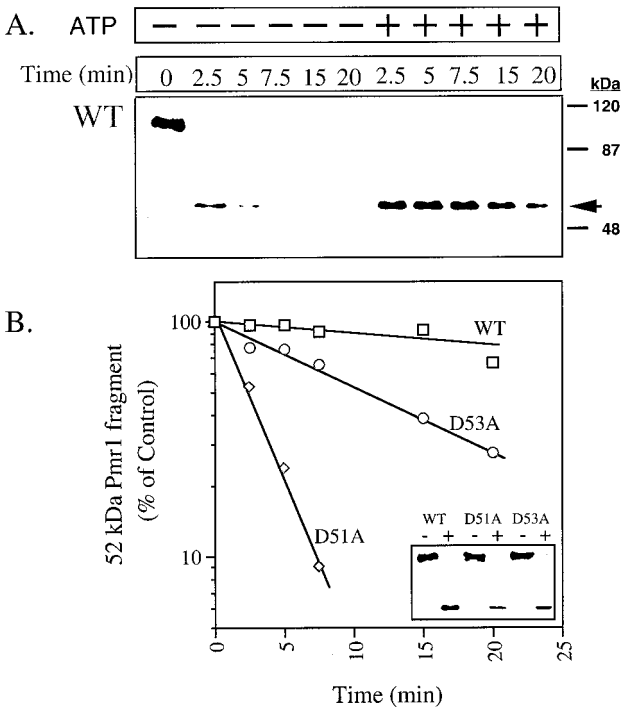

FIGURE 9: Trypsinolysis of Pmr1 polypeptides. (Panel A) Golgi membranes, containing $(His)_9$-tagged Pmr1, were subjected to limited digestion with trypsin for the times shown, under the conditions described under Experimental Procedures. The topmost panel indicates the addition of 5 mM ATP, prior to trypsin addition. Membranes were separated by SDS−PAGE and immunoblotted using polyclonal anti-Pmr1 antibodies, raised against a fusion of the C-terminal one-third of Pmr1 and bacterial TrpE (*11*). The arrow points to the ATP-protectable fragment at a molecular mass of 52 kDa, as judged by the migration of molecular mass markers, indicated on the extreme right. (Panel B) Time course of digestion of the 52 kDa Pmr1 fragment in the presence of ATP. Western blots showing the tryptic fragments generated by digestion of wild-type (panel A) or mutant membranes (not shown) were scanned and quantitated using MacBAS v2.31. Amounts shown are expressed as a percentage of the undigested full-length control Pmr1 polypeptide, and data points were fitted by linear regression. Inset: Western blot of membranes from wild type or mutant, as indicated, in the absence (−) or presence (+) of ATP and trypsin, incubated for 2.5 min.

mutants, similar to the loss of Ca^{2+} transport observed in Golgi fractions (Figure 4A). The D51A substitution caused a significant decrease in Mn^{2+} tolerance, suggesting a reduction in Mn^{2+} transport consistent with a reduction in Ca^{2+} transport (decreased V_{max} and affinity) in this mutant. In contrast, the D53A and D51,53A mutants were indistinguishable in Mn^{2+}-tolerant growth from the wild-type control. This was surprising, particularly for the double mutant, which had only low levels of Ca^{2+} transport activity. It is possible that the double mutant may be active in sequestering Mn^{2+} in the endoplasmic reticulum, where it is largely retained, despite our inability to detect Ca^{2+} pumping activity in ER-containing fractions of the sucrose gradient. The data suggest that the D53A substitution retains or enhances Mn^{2+} transport, despite a diminution in Ca^{2+} transport.

To further explore the ion specificity of the mutants, we assessed the ability of Mn^{2+} ions to compete with ^{45}Ca transport in Golgi fractions (Figure 8). In wild type, Mn^{2+} was a potent inhibitor of ^{45}Ca transport, with half-maximal inhibition occurring at 0.2 μM free Mn^{2+}, under conditions where ^{45}Ca was approximately 10-fold in excess of the K_M for Ca^{2+} (0.8 μM; see Experimental Procedures). These data suggest that Pmr1 is selective for Mn^{2+} ions over Ca^{2+}. Under identical conditions, the D51A mutation displayed a $K_{0.5}$ for Mn^{2+} ions of 1.7 μM, an 8-fold increase similar to the change in the K_M for Ca^{2+} transport. In contrast, the D53A mutation slightly *decreased* the $K_{0.5}$ for Mn^{2+} ions to 0.09 μM, strongly suggesting that this mutant has an increased affinity for transport of Mn^{2+} ions, relative to Ca^{2+}.

N-Terminal Mutations Alter the Stability of the C-Terminal Half of the Polypeptide. Limited trypsinolysis can be used to probe polypeptide folding, and to monitor conformational changes upon substrate binding. Golgi membranes from control or *pmr1* mutant strains were subjected to digestion by trypsin, as described under Experimental Procedures, in the absence or presence of ATP. Western blots of the digested membranes were probed with polyclonal antibodies, raised against the C-terminal third of Pmr1, including the ATP-binding domain (*11*). The 105 kDa Pmr1 polypeptide undergoes rapid cleavage to a 52 kDa intermediate that is significantly stabilized in the presence of ATP (Figure 9 A). The trypsin-sensitive site in Pmr1 is likely to be in the vicinity of the T_1 cleavage site described for the related SERCA pump, approximately halfway within the protein sequence (*24*). Trypsinolysis of the single and double point mutants (Figure 9B), and of the ΔEF16 deletion mutant (not shown), revealed an identical pattern of cleavage, including ATP stabilization of the 52 kDa intermediate, indicating that the gross conformation of the polypeptide was unaltered by the mutations. Substitution of either of the aspartates had a destabilizing effect on the 52 kDa polypeptide, suggestive of long-range conformational coupling between the two distal parts of the protein. However, it was noteworthy that the D51A mutation had a much greater destabilizing effect on the ATP-binding proteolytic intermediate, relative to the D53A mutation (Figure 9B). This is striking, since both mutations had similar effects on biogenesis and trafficking to the Golgi, suggesting an overall similarity in protein

folding and stability. Furthermore, because the D51A mutation had a significantly smaller effect on the K_M for Ca^{2+} (Figure 6), a general, nonspecific destabilizing effect of this mutation on protein stability seems unlikely. We propose, from these experiments, that the N-terminal domain of Pmr1 interacts with the C-terminal ATP-binding regions of the protein to influence proteolytic stability, and that alterations within the N-terminal Ca^{2+}-binding motif are transmitted to the catalytic domain.

DISCUSSION

P-type ATPases have been subjected to extensive mutagenesis, as exemplified by the >200 site-directed mutations in the sarco/endoplasmic reticulum Ca^{2+}-ATPase (reviewed in refs *4*, *25*). Major advances stemming from this work have been the identification of cation-binding residues and inhibitor sites within the transmembrane domains. Notably, mutagenesis of the cytoplasmic N-terminal segment of SERCA has not yielded information relevant to a functional role for this domain in Ca^{2+} transport. However, the identification of metal-binding sites within the N-terminus of the soft metal-transporting ATPases (Cu^{2+}-, Zn^{2+}-, Hg^{2+}-, Cd^{2+}-ATPases) implicates this region in either modulating or participating in ion transport. The presence of a putative Ca^{2+}-binding motif within the N-terminus of Pmr1, the yeast Golgi Ca^{2+}-ATPase, provided an opportunity to investigate the role of ion binding sites distal to the transmembrane pore. Yeast mutant strains, with low endogenous pump activity, have proven to be ideal for transport studies of Pmr1 (*11*), as well as for the heterologous expression of Ca^{2+} pumps from plants and animals (*26*, *27*).

The canonical EF hand motif, originally described by Kretsinger and colleagues (*28*), has two cooperatively interacting domains, each of which consists of two perpendicularly placed α-helices (termed E and F) connected by an ion-binding loop. The unpaired EF hand motif, as seen in Pmr1, although less well studied, is not without precedence. For example, Ca^{2+} binding by an unpaired EF hand-like motif has been reported for the HIV-1 envelope protein gp41 (*29*) and the vitronectin receptor (*30*). We note that sequence analysis of more than 160 binding loops demonstrates that there is no simple relationship between loop sequence and the affinity or specificity of ion binding, and that the structural context and variability of noncoordinating residues must also be taken into account (*32*). Thus, visual inspection of a sequence is not a reliable prediction of Ca^{2+} binding. The first question we considered, therefore, was whether the EF hand-like motif of Pmr1 has Ca^{2+}-binding ability. Here, we provide direct evidence that the N-terminal 75 amino acids of Pmr1 fused with glutathione-*S*-transferase bind Ca^{2+}, and that a mutation at Asp53 within the predicted EF hand-like motif alters Ca^{2+} binding.

A second question fundamental to this study was whether the N-terminal Ca^{2+}-binding motif in Pmr1 is essential for Ca^{2+} transport. The complete loss of transport activity in the four deletion mutants would suggest that it is, although it is difficult to rule out a nonspecific effect caused by structural derangements. However, it is clear that the overall structure of the mutant proteins was preserved, since we observed ATP-protectable tryptic fragments identical to that of wild type. In contrast, we note that grossly misfolded protein resulted from the substitution of the phosphorylated aspartate in the related yeast H^+-ATPase, Pma1, as judged by a dominant negative phenotype, complete retention of the mutant polypeptide in the endoplasmic reticulum, hypersensitivity to trypsin, and absence of ligand-protectable tryptic fragments (*33*).

Introduction of the D51A and D53A mutations within the N-terminal EF hand-like motif had distinct functional effects that were both novel and mechanistically intriguing. First, mutations within the N-terminal Ca^{2+}-binding motif increased the apparent K_M for Ca^{2+} transport substantially: 8-fold for the D51A mutation and 11-fold for the D53A mutation. It is particularly noteworthy that all of the mutations in SERCA that significantly altered the affinity for Ca^{2+} (>3-fold) were located within transmembrane domains. Thus, over 200 point mutations in the extramembranous regions of SERCA were reported that did not alter the affinity for Ca^{2+} transport. In this context, the observed effects of the Pmr1 mutations appear to be both specific and significant. Second, the two mutations had differential effects on transport of Ca^{2+} (as measured by the K_M for Ca^{2+}), versus Mn^{2+} (as inferred from Mn^{2+} tolerant growth and Mn^{2+} inhibition of Ca^{2+} transport). Thus, replacement of the aspartate at position 51 was less deleterious to Ca^{2+} transport than the corresponding substitution at position 53. On the other hand, the D51A mutant showed reduced tolerance to Mn^{2+} ions, whereas the D53A mutation did not. We conclude that the mutations have differential effects on ion selectivity. Third, the two EF hand mutations altered the stability of the C-terminal half of the ATPase, to widely different extents. While it is recognized that a point mutation may exert a nonspecific destabilizing effect on the entire polypeptide, it is remarkable that mutations separated by one residue could have such strikingly different effects. The similarities in expression levels, Golgi targeting, and V_{max} for Ca^{2+} transport between the two substitutions argue against nonspecific effects of the D51A mutation on the stability of the ATP-binding proteolytic fragment of the pump. Taken together, the data suggest that the N-terminal domain interacts with the C-terminal half of the ATPase, and that this interaction mediates the effects on ion transport observed in this study.

To explain the modulatory effects of the N-terminal domain on ion transport, we propose a working model in which high-affinity cation (calcium or manganese) binding by the EF hand-like domain is required for activation of the Pmr1 pump, likely via interaction with the catalytic nucleotide-binding domain. The complete loss of transport observed in the deletion mutants is consistent with this model, although we cannot rule out structural perturbations in these mutants. We suggest that substitution of the aspartates at positions 51 and 53 alters the affinity and ion selectivity of the N-terminal site, resulting in concomitant changes in activation of the pump. Thus, the observed shifts in the affinity for calcium or manganese transport might be a reflection of the titration of the N-terminal ion binding site, and of pump activation, rather than a titration of the transport site. This model predicts that the D51A mutation does not alter the selectivity of the site, while the D53A mutation increases the selectivity for Mn^{2+} over Ca^{2+}. The double mutation would be expected to be intermediate in ion-binding properties. In the wild-type pump, the affinity of the modulatory site for Ca^{2+} and Mn^{2+} would be predicted to

be higher than that of the transport site.

In conclusion, we show here that an N-terminal EF hand-like motif in Pmr1 binds Ca^{2+} and that alterations to this cation-binding site modulate pump activity and ion affinity. A clarification of the mechanism of this modulation will require a quantitative analysis of the properties of the N-terminal ion-binding site.

ACKNOWLEDGMENT

We thank Dr. Gerda Breitwieser for productive discussions and for critical reading of the manuscript.

REFERENCES

1. Lutsenko, S., and Kaplan, J. H. (1995) *Biochemistry 34*, 15607−15613.
2. Auer, M., Scarborough, G. A., and Kuhlbrandt, W. (1998) *Nature 392*, 840−843.
3. Zhang, P., Toyoshima, C., Yonekura, K., Green, N. M., and Stokes, D. L. (1998) *Nature 392*, 835−839.
4. MacLennan, D. H., Rice, W. J., and Odermatt, A. (1997) *Ann. N.Y. Acad. Sci. 834*, 175−185.
5. Clarke, D. M., Loo, T. W., and MacLennan, D. H. (1990) *J. Biol. Chem. 265*, 14088−14092.
6. Enyedi, A., Vorherr, T., James, P., McCormick, D. J., Filoteo, A. G., Carafoli, E., and Penniston, J. T. (1989) *J. Biol. Chem. 264*, 12313−12321.
7. Portillo, F., Eraso, P., and Serrano, R. (1991) *FEBS Lett. 287*, 71−74.
8. Vulpe, C., Levinson, B., Whitney, S., Packman, S., and Gitschier, J. (1993) *Nat. Genet. 3*, 7−13.
9. Payne, A. S., and Gitlin, J. D. (1998) *J. Biol. Chem. 273*, 3765−3770.
10. Rudolph, H. K., Antebi, A., Fink, G. R., Buckley, C. M., Dorman, T. E., LeVitre, J., Davidow, L. S., Mao, J. I., and Moir, D. T. (1989) *Cell 58*, 133−145.
11. Sorin, A., Rosas, G., and Rao, R. (1997) *J. Biol. Chem. 272*, 9895−9901.
12. Ikura, M. (1996) *Trends Biochem. Sci. 21*, 14−17.
13. Xiong, H., Feng, X., Gao, L., Pasek, D. A., Seok, J. H., and Meissner, G. (1998) *Biochemistry 37*, 4804−4814.
14. Czempinski, K., Zimmerman, S., Ehrhardt, T., and Muller-Rober, B. (1997) *EMBO J. 16*, 2565−2575.
15. Cunningham, K. W., and Fink, G. R. (1994) *J. Cell Biol. 124*, 351−363.
16. Sarkar, G., and Sommer, S. S. (1990) *BioTechniques 8*, 404−407.
17. Barik, S., and Galinsky, M. S. (1991) *BioTechniques 10*, 489−490.
18. Fabiato, A., and Fabiato, F. (1979) *J. Physiol. 75*, 463−505.
19. Lundberg, S., Bjork, J., Lofvenberg, L., and Backman, L. (1995) *Eur. J. Biochem. 230*, 658−665.
20. Lowry, O. H., Rosebrough, N. J., Farr, A. L., and Randall, R. J. (1951) *J. Biol. Chem. 193*, 265−275.
21. Nakamoto, R. K., Rao, R., and Slayman, C. W. (1991) *J. Biol. Chem. 266*, 7940−7949.
22. Lapinskas, P. J., Cunningham, K. W., Liu, X. F., Fink, G. R., and Culotta, V. C. (1995) *Mol. Cell. Biol. 15*, 1382−1388.
23. Durr, G., Strayle, J., Plemper, R., Elbs, S., Klee, S. K., Catty, P., Wolf, D., and Rudolph, H. K. (1998) *Mol. Biol. Cell 9*, 1149−1162.
24. Stewart, P. S., MacLennan, D. H., and Shamoo, A. E. (1976) *J. Biol. Chem. 251*, 712−719.
25. Andersen, J. P., and Vilsen, B. (1995) *FEBS Lett. 359*, 101−106.
26. Liang, F., and Sze, H. (1998) *Plant Physiol. 118*, 817−825.
27. Degand, I., Catty, P., Talla, E., Thines-Sempoux, D., d'Exaerde, A., Goffeau, A., and Ghislain, M. (1999) *Mol. Microbiol. 31*, 545−556.
28. Kretsinger, R. H., and Kockolds, C. E. (1973) *J. Biol. Chem. 248*, 3313−3326.
29. Ebenbichler, C. F., Stoiber, H., Schneider, R., Patsch, J. R., and Dierich, M. P. (1996) *J. Virol. 70*, 1723−1728.
30. Edwards, J. G., Hameed, H., and Campbell, G. (1988) *J. Cell Sci. 89*, 507−513.
31. Loukin, S., and Kung, C. (1995) *J. Cell Biol. 131*, 1025−1037.
32. da Silva, A. C. R., and Reinach, F. C. (1991) *Trends Biochem. Sci. 16*, 53−57.
33. Nakamoto, R. K., Verjovski-Almeida, S., Allen, K. E., Ambesi, A., Rao, R., and Slayman, C. W. (1998) *J. Biol. Chem. 273*, 7388−7344.
34. Strausak, D., La Fontaine, S., Hill, J., Firth, S. D., Lockhart, P. J., and Mercer, J. F. B. (1999) *J. Biol. Chem. 274*, 11170−11177.

BI9911233